A&A 421, 241–254 (2004)
DOI: 10.1051/0004-6361:20041042

Astronomy & Astrophysics

Precise radial velocity measurements of G and K giants⋆

Multiple systems and variability trend along the Red Giant Branch

J. Setiawan[1,5], L. Pasquini[2], L. da Silva[3], A. P. Hatzes[4], O. von der Lühe[5], L. Girardi[6], J. R. de Medeiros[7], and E. Guenther[4]

[1] Max-Planck-Institut für Astronomie, Koenigstuhl 17, 69117 Heidelberg, Germany
[2] European Southern Observatory, Karl-Schwarzschild-Str. 3, 85748 Garching bei München, Germany
[3] Observatório Nacional, R. Gal. José Cristino 77, 20921-400 Sao Cristavao, Rio de Janeiro, Brazil
[4] Thüringer Landessternwarte Tautenburg, Sternwarte 5, 07778 Tautenburg, Germany
[5] Kiepenheuer-Institut für Sonnenphysik, Schoeneckstr. 6, 79104 Freiburg (Brsg), Germany
[6] Osservatorio Astronomico di Trieste, via Tiepolo 11, 34131 Trieste, Italy
[7] Departamento de Física, Universidade Federal do Rio Grande do Norte, 59072-970 Natal, Brazil

Received 15 January 2004 / Accepted 14 March 2004

Abstract. We present the results of our radial velocity (RV) measurements of G and K giants, concentrating on the presence of multiple systems in our sample. Eighty-three giants have been observed for 2.5 years with the fiber-fed echelle spectrograph FEROS at the 1.52 m ESO telescope in La Silla, Chile. Seventy-seven stars (93%) of the targets have been analyzed for RV variability using simultaneous Th–Ar calibration and a cross-correlation technique. We estimate the long-term precision of our measurement as better than 25 m s^{-1}. Projected rotational velocities have been measured for most stars of the sample. Within our time-base only 21 stars (or 27%) show variability below 2σ, while the others show RV variability with amplitudes up to several km s^{-1}. The large amplitude (several km s^{-1}) and shape (high eccentricity) of the RV variations for 11 of the program stars are consistent with stellar companions, and possibly brown dwarf companions for two of the program stars. In those systems for which a full orbit could be derived, the companions have minimum masses from ~0.6 $M_{\odot}$ down to 0.1 $M_{\odot}$. To these multiple systems we add the two candidates of giant planets already discovered in the sample. This analysis shows that multiple systems contribute substantially to the long-term RV variability of giant stars, with about 20% of the sample being composed of multiple systems despite screening our sample for known binary stars. After removing binaries, the range of RV variability in the whole sample clearly decreases, but the remaining stars retain a statistical trend of RV variability with luminosity: luminous cool giants with $B - V \geq 1.2$ show RV variations with $\sigma_{\overline{\mathrm{RV}}} > 60$ m s^{-1}, while giants with $B - V < 1.2$ including those in the clump region exhibit less variability or they are constant within our accuracy. The same trend is observed with respect to absolute visual magnitudes: brighter stars show a larger degree of variability and, when plotted in the RV variability vs. magnitude diagram a trend of increasing RV scatter with luminosity is seen. The amplitude of RV variability does not increase dramatically, as predicted, for instance, by simple scaling laws. At least two luminous and cooler stars of the sample show a correlation between RV and chromospheric activity and bisector asymmetry, indicating that in these two objects RV variability is likely induced by the presence of (chromospheric) surface structures.

Key words. stars: variables: general – stars: binaries: general – stars: late-type – stars: rotation – technique: radial velocities

1. Introduction

Precise RV measurements have been the subject of strong interest in the last years, thanks mostly to their successful application to the detection of planetary companions orbiting solar-type stars (Mayor & Queloz 1995; Marcy & Butler 1996). Long-term precision better than 10 m s^{-1} is required to detect Jovian planets orbiting a dwarf star at 5 AU. Evolved cool stars (hereafter "giants") show a higher level of RV variability (see e.g., Walker et al. 1989; Hatzes & Cochran 1993) and for them such a high long-term precision may not be required, although G-type, low luminous sub-giants which are not very different from solar-type stars may exhibit RV variability as low as a few tens of m s^{-1}, as presented in our results (see Sect. 4.2)

Precise RV measurements have also been applied to the study of stellar pulsations, e.g. solar-type oscillations, in which a short-term accuracy of better than 1 m s^{-1} is needed to

Send offprint requests to: J. Setiawan,
e-mail: setiawan@mpia-hd.mpg.de

⋆ Based on observations collected at the 1.52 m-ESO telescope at the La Silla Observatory from Oct 1999 to Feb. 2002 under ESO programs and the ESO-Observatório Nacional, Brazil, agreement and in part on observations collected on the Alfred Jensch 2 m telescope of the Thüringer Landessternwarte Tautenburg.

detect p-modes. Solar-type pulsations have so far been detected on Procyon (Brown et al. 1991; Barban et al. 1999), β Hydri (Bedding et al. 2001) and α Cen A (Bouchy & Carrier 2001). Until now, the only "solar-like" oscillations in a giant star have been detected by Frandsen et al. (2002) in ξ Hya (spectral class G7III). The oscillation period was $P = 2$–5.5 h. Other evidence for p-mode oscillations in K giants with period of several days have been detected in Arcturus (Hatzes & Cochran 1994; Merline et al. 1995) and in α UMa (Buzasi et al. 2000).

To achieve high precise RV two techniques are currently in use: acquiring a simultaneous calibration for the stellar spectra (Baranne et al. 1996) or the self absorption-cell technique (Campbell & Walker 1979; Cochran & Hatzes 1990). Both techniques are presently able to provide comparable long-term precision of a few m s^{-1} (Butler et al. 1996; Pepe et al. 2000).

G and K giants are cool, evolved stars, which have moved off the main sequence. They span the entire Red Giant Branch (RGB) including the red clump and early-AGB phases. The clump giants are stars which are experiencing the He-core burning phase.

RV variations of K giants with amplitudes between 30–300 m s^{-1} and time-scales ranging from a few to hundreds of days have been reported by Smith et al. (1987), Walker et al. (1989), Larson et al. (1993), Hatzes & Cochran (1993, 1996). The RV variability observed in red giants has been suggested to result from stellar pulsation, rotational modulation, or low-mass companion. Before we started to publish the results of this survey a few sub-stellar companions have been proposed around evolved stars: the K4IVa sub-giant HD 27442 (Butler et al. 2001), the K2III giant ι Dra (Frink et al. 2002) and γ Cephei (Hatzes et al. 2003). We have enlarged this sample by detecting two giant planet candidates around HD 47536 (Setiawan et al. 2003b) and HD 122430 (Setiawan 2003c). Recently, Sato et al. (2003) reported the first detection of a planetary companion to a G giant, HD 104985. The search of extra-solar planets around giants is quite interesting and complementary to the surveys carried out on main sequence stars: giants in fact may cover a range of stellar masses. Stars with masses exceeding 3–4 $M_{\odot}$ cannot be investigated for the presence of low-mass companions while on the main sequence because they have fewer stellar absorption lines due to a higher effective temperature. Furthermore, early-type stars have broad spectral features due to the more rapid rotation compared to late-type stars. Both effects severely limit the accuracy of RV measurements. As an early-type star evolves off the main sequence its rotation rate slows considerably (Pasquini et al. 2000; de Medeiros & Mayor 1999) and the atmosphere cools. The larger number of narrow absorption lines now makes these objects suitable objects for precise RV studies.

Most of the previous RV results were obtained on relatively smaller samples of giants. We have therefore recognized the need for a RV survey of G and K giants spanning the entire RGB: 1) to determine how the RV variations vary as a star moves along the RGB, and 2) to understand the nature of the long-period variations. If these variations were due to rotational modulation of stellar surface structure, then our survey would provide the ideal targets for stellar interferometers, since many of these objects have angular diameters which are large enough to be resolved by long-baseline interferometry.

Our first work mostly concentrated on the description of the observations and the data reduction techniques and summarized the first results. These showed that some relation was likely to be present between the RV variation amplitudes and the position of the stars in the H-R diagram (Setiawan et al. 2003a, hereafter Paper I). In the present work we will concentrate on the detection of multiple systems. These systems need to be recognized and separated by the rest of the sample stars before the other causes of variability are investigated.

2. Observations

Sixty-five nights (ESO-time and Brazilian Observatório Nacional-time) were allocated from October 1999 to February 2002 to this program on FEROS, the echelle spectrograph at the 1.52 m-ESO telescope in La Silla. The spectrograph provides a full wavelength coverage of 3500–9200 Å over 39 spectral orders at a resolving power $\lambda/\Delta\lambda$ of 48 000 (Kaufer & Pasquini 1998). This enabled us to record simultaneously the portion of the spectrum used for RV determinations as well as chromospheric activity indicators like the Ca II H and K lines. FEROS is equipped with a double fiber system, one for the object and a second fiber which can record the sky or a simultaneous wavelength calibration, which can be used for accurate RV determination (Baranne et al. 1996).

The RV precision achieved with FEROS during commissioning was 23 m s^{-1} (Kaufer & Pasquini 1998) and could be reduced on a short (few months) time-scale to better than 11 m s^{-1} using an improved data reduction method (Setiawan et al. 2000, and Paper I). Unfortunately, this precision could not be maintained until the end of our survey. We detected instrumental instabilities which affected the simultaneous Th–Ar calibration. Our precision over 28 months is better than 25 m s^{-1}, similar to the commissioning accuracy and still appropriate for our scientific goals.

The program started with 27 stars in October 1999 and has been expanded to include 83 G and K stars, mainly giants. The whole sample covers a large fraction of the upper H-R diagram including the full RGB as well as the "clump" region (cf. Fig. 1). The bulk of our sample has been selected on the basis of HIPPARCOS parallaxes and are not classified as spectroscopic binaries. A few stars with measured $v_{\rm rot} \sin i$ have been added later to be used as comparison with our $v_{\rm rot} \sin i$ calibration. Some of these stars are binaries.

Being interested in abundances, variability in Ca II H and K core emission lines and bisector variations, we required an average signal to noise ratio (S/N) of about 150–200 per pixel in the best exposed part of the spectra. We found this high S/N is appropriate for investigating the variations of the deep Ca II K (λ = 3934 Å) line, the best indicator of chromospheric activity (see e.g. Pasquini et al. 1990). More details about the observation and the calibration procedure were presented in Paper I and are only briefly repeated here.

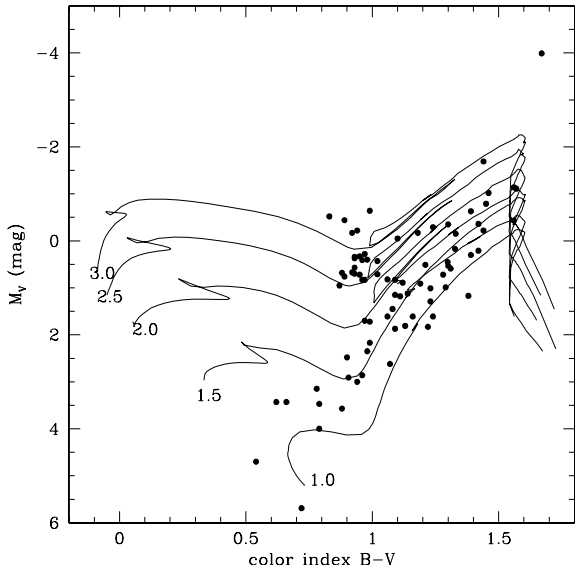

Fig. 1. H-R diagram of the 83 giant stars in our RV survey with FEROS. The sample covers the RGB including the "clump" region. The continuous lines are evolutionary tracks for solar-metallicity stars of masses comprised between 1.0 and 3.0 $M_\odot$, taken from Girardi et al. (2000).

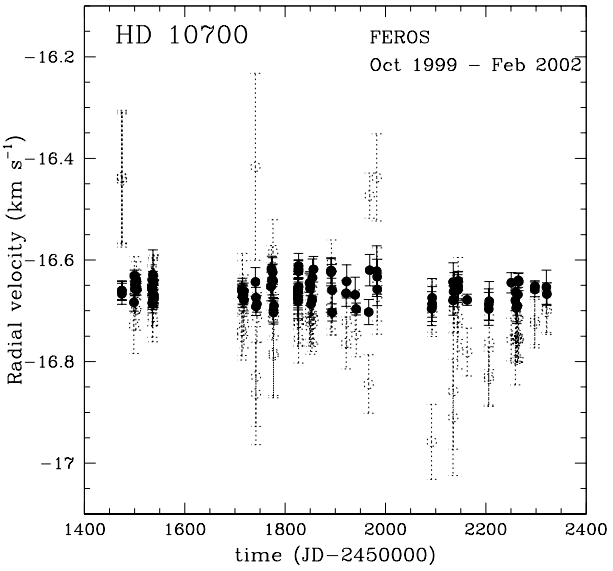

Fig. 2. RV plot of τ Cet (HD 10700) during the 2.5 years observation, the open circles represent the RV computation by the original method, the full filled circle are the final corrected RV. The final precision determined for FEROS during our survey is 22.8 m s^{-1}.

3. Data analysis

3.1. Radial velocity computation

The RV computation was carried out with the TACOS package, developed by the Geneva observatory, using a cross-correlation routine, which operates on one-dimensional order spectra with a numerical template (*mask*), e.g. stellar mask for fiber 1, thorium (Th) mask for fiber 2 as well as for calibration exposures (*double Th–Ar*). The resulting cross-correlation function (CCF) is then fitted with a Gaussian. While the position of the maximum of the Gaussian fit is used for RV determination, the width $\sigma_{\rm CCF}$ can be used to compute the projected rotational velocity $v_{\rm rot} \sin i$ as demonstrated in Queloz et al. (1998). The result of $v_{\rm rot} \sin i$ computation is presented in Sect. 3.2.

Due to instrumental systematic instabilities we had to apply RV corrections using the procedure presented in Paper I. Figure 2 shows a comparison between the original RV computation method (dashed open circles) and the RV obtained after the corrections (dots) for our standard "constant" star τ Cet (HD 10700). The standard deviation of the corrected τ Cet radial velocities is $\sigma_{\overline{\rm RV},\tau\,{\rm Cet}} = 22.8$ m s^{-1} which we use as an estimate of our long-term RV (instrumental) precision. This value is three times worse than reported in Setiawan et al. (2000) and substantially higher than in Paper I. We have tried several weighting methods (e.g. by σ, σ^2 or by flux in the center of order) when combining the RV of each order to obtain the mean RV of a single spectrum, but these efforts did not improve the final result. We cannot exclude that it may be possible to improve our precision, for instance by using different masks or improving the wavelength calibration. It is nevertheless worrying that our precision substantially decreased during the second and third years of observations. We do not have a clear-cut explanation for this. However, we noticed that over time the FEROS environment and optical alignment deteriorated and this could be a cause of the degraded RV performances. The original specifications for FEROS were 50 m s^{-1}, which were at all times fulfilled. A precision of ∼25 m s^{-1} is slightly worse than our goal, but is appropriate for analyzing the long-term variability of the sample; most of our targets show typical RV variability of $\sigma_{\overline{\rm RV}} \geq 50$ m s^{-1}.

3.2. Projected rotational velocity v_{rot} sin i

Since one of the possible sources of RV variation is stellar surface inhomogeneities (e.g. spots) it is important to derive rotational velocities for the sample stars which can be used with measurements (estimates) of the stellar radii to derive upper limits to the stellar rotational period. These can then be compared to the RV period derived from a periodogram analysis. We used the cross-correlation method (see Queloz et al. 1998) to determine the projected rotational velocity $v_{\rm rot} \sin i$ from the width $\sigma_{\rm CCF}$ of the stellar CCF. Melo et al. (2001) determined the calibration value for FEROS and applied it to compute $v_{\rm rot} \sin i$ of giants in the M 67 cluster.

By using the cross-correlation technique the rotational velocity can be expressed by the relation (Benz & Mayor 1984; Queloz et al. 1998):

$$v_{\rm rot} \sin i = A \sqrt{\sigma^2_{\rm CCF} - \sigma^2_0}, \quad (1)$$

where A is a constant and σ_0 depends on the instrumental resolution and the intrinsic width of the stellar line without rotation (e.g. macroturbulence). The latter will depend on the stellar effective temperature and gravity (cf. Gray 1976). Following the Melo et al. (2001) calibration we adopted

$$\sigma_0 = 0.417(B-V)^2 + 4.225 \quad (2)$$

Table 1. Projected rotational velocity and RV variation of G and K giants/sub-giants. Column (1): identifer, Col. (2): absolute magnitude; Col. (3): color index; Col. (4): visual magnitude; Col. (5): spectral classification (SIMBAD); Col. (6): CCF width; Col. (7): σ_0 from Eq. (2); Col. (8): projected rotational velocity from FEROS and Col. (9) other measurements; Col. (10): available reference for $v_{\rm rot} \sin i$; Col. (11): rms of RV variation; Col. (12): number of spectra.

HD	M_V	$B-V$	m_V	Spectral type	$\sigma_{\rm CCF}$ km s^{-1}	σ_0 km s^{-1}	$v_{\rm rot} \sin i$ km s^{-1} FEROS	$v_{\rm rot} \sin i$ km s^{-1} other	Ref.	$\sigma_{\overline{\rm RV}}$ m s^{-1}	N
2114	−0.52	0.83	5.78	G5III	5.19	4.51	4.9	3.9	(a)	63	5
2151	3.43	0.62	2.80	G2IV	5.12	4.39	5.0			39	5
7672	0.96	0.87	5.42	G5III	5.34	4.54	5.3	4.5	(a)	2011	9
10 700	5.69	0.72	3.50	G8V	4.55	4.44	1.9			23	105
10 761	−0.22	0.94	4.27	K0III	4.84	4.60	2.9	2.9	(a)	76	7
11 977	0.57	0.93	4.68	G5III	4.76	4.59	2.4			70	53
12 438	0.68	0.88	5.34	G8III	4.85	4.55	3.2			57	61
16 417	3.43	0.66	5.79	G5IV	4.79	4.41	3.6			45	71
18 322	0.83	1.09	3.89	K1III	4.75	4.72	1.1			53	75
18 885	1.15	1.09	5.84	G6III	4.81	4.72	1.7			53	51
18 907	3.47	0.79	5.89	G5IV	4.58	4.49	1.7			60	51
21 120	−0.44	0.89	3.62	K1IV/V	5.71	4.55	6.6	5.9	(c)	1346	6
22 663	0.43	1.02	4.57	K0III	4.72	4.66	1.4			954	44
23 319	0.91	1.19	4.59	K2III	4.88	4.82	1.4			48	53
23 940	0.83	0.97	5.52	G6III	5.46	4.62	5.5			47	43
26 923	4.70	0.54	6.33	G0IV	4.77	4.35	3.7	4.3	(c)	69	7
27 256	−0.17	0.92	3.33	G7III	5.59	4.57	6.1			136	56
27 371	0.28	0.97	3.65	K0III	4.84	4.62	2.7	2.4	(a)	54	32
27 697	0.40	0.98	3.76	K0III	4.97	4.63	3.4	2.5	(a)	1794	32
32 887	−1.02	1.46	3.19	K4III	4.94	5.11	−−			60	63
34 642	2.17	0.99	4.81	K1III	4.67	4.63	1.2			43	44
36 189	−0.64	0.99	5.14	G6III	5.69	4.63	6.3			48	36
36 848	1.83	1.22	5.45	K2III	4.64	4.85	−−			47	46
40 176	−0.05	1.10	4.97	K1III	4.92	4.73	2.6			4078	41
47 205	2.47	1.05	3.96	K1III	4.52	4.68	−−			−−	<4
47 536	−0.17	1.18	5.25	K1III	4.91	4.80	1.9			76	38
50 778	−0.36	1.42	4.08	K4III	4.96	5.06	−−			97	46
61 935	0.71	1.02	3.94	K0III	4.76	4.66	1.9			55	44
62 644	3.15	0.78	5.06	G5IV	4.71	4.48	2.8			4486	30
62 902	1.17	1.38	5.49	K5III	4.74	5.02	−−			57	33
63 697	0.72	1.28	5.17	K3III	4.74	4.91	−−			54	30
65 695	0.51	1.21	4.93	K2III	4.87	4.83	1.2			66	29
65 735	1.18	1.11	6.30	K1III	4.86	4.74	2.0	1.0	(c)	43	17
70 982	0.34	0.93	6.11	G8III	5.10	4.59	4.3	3.3	(e)	43	17
72 650	0.39	1.36	6.34	K3III	4.75	5.00	−−	1.8	(e)	61	18
78 647	−3.99	1.67	2.23	K4II	6.43	5.38	6.7	5.6	(e)	301	34
81 361	1.70	0.97	6.30	G9III	4.62	4.62	<1			49	7
81 797	−1.69	1.44	1.99	K3III	5.12	5.09	1.1	<1.4	(b)	63	40
83 441	0.89	1.12	5.96	K2III	4.75	4.75	<1			115	27
85 035	2.62	1.07	7.02	K1III	4.58	4.70	−−			46	9
90 957	0.21	1.42	5.58	K3III	4.81	5.07	−−			52	22
92 588	3.57	0.88	6.25	K1IV	4.61	4.55	1.4	1.0	(c)	34	19
93 257	1.81	1.13	5.50	K3III	4.64	4.76	−−			29	20
93 773	0.72	0.95	6.51	G8III	4.80	4.60	2.6			77	18
99 167	−0.43	1.56	4.81	K5III	5.03	5.23	−−			94	30
10 1321	1.72	0.99	6.80	K0III	4.64	4.63	<1			70	15
107 446	−0.63	1.39	3.59	K4III	4.94	5.03	−−			85	33
108 570	3.00	0.94	6.13	K1III	4.60	4.59	<1			71	4
110 014	−0.29	1.24	4.66	K2III	5.02	4.87	2.3			92	26

and $A = 1.9 \pm 0.1$. Our $v_{\rm rot} \sin i$ are given in Table 1. The uncertainty in the $v_{\rm rot} \sin i$ determination is about 1 km s^{-1} and is mostly due to calibration Eq. (2), which assumes that σ_0 is the same for all the stars with the same color. This assumption may be reasonable for stars where the dominant broadening mechanism is rotation, but can result in larger errors for stars with low

Table 1. continued.

HD	M_V	$B-V$	m_V	Spectral type	σ_{CCF} km s^{-1}	σ_0 km s^{-1}	$v_{rot}\sin i$ km s^{-1} FEROS	$v_{rot}\sin i$ km s^{-1} other	Ref.	$\sigma_{\overline{RV}}$ m s^{-1}	N
111 884	0.59	1.31	5.91	K3III	4.77	4.94	−−			37	20
113 226	0.37	0.93	2.85	G8III	4.99	4.59	3.7	3.2	(d)	43	35
115 439	0.38	1.34	6.05	K3III	4.80	4.97	−−	1.0	(e)	−−	<4
115 478	0.53	1.30	5.33	K3III	4.75	4.93	−−			73	26
121 416	1.12	1.14	5.82	K1III	4.82	4.77	1.3			37	9
122 430	−0.15	1.33	5.47	K3III	4.82	4.96	−−			81	25
124 882	−0.35	1.30	4.31	K2III	4.82	4.93	−−			57	26
125 560	1.01	1.23	4.84	K3III	4.87	4.85	<1	1.0	(c)	49	23
131 109	−0.22	1.44	5.37	K4III	4.87	5.09	−−			70	23
131 977	6.88	1.11	5.74	K4V	4.71	4.74	−−			86	9
136 014	0.83	0.96	6.19	G8III	5.30	4.61	5.0			75	20
148 760	1.87	1.09	6.07	K1III	4.74	4.72	<1			60	20
151 249	−1.14	1.56	3.77	K5III	5.09	5.24	−−			281	28
152 334	0.30	1.39	3.62	K4III	4.77	5.03	−−			42	29
152 980	−0.79	1.45	4.06	K4III	5.00	5.10	−−			66	26
156 111	4.00	0.79	7.22	G8V	4.60	4.48	2.0			1954	16
159 194	1.61	1.24	6.76	K3III	4.80	4.87	−−			88	25
165 760	0.33	0.95	4.64	G8III	4.86	4.60	3.0	3.9/2.2	(a)/(c)	55	29
169 370	1.61	1.16	6.28	K0	4.74	4.79	−−			54	23
174 295	0.41	0.96	5.18	K0III	4.83	4.61	2.7			54	25
175 751	0.82	1.06	4.83	K1III	4.76	4.69	1.5			49	31
176 578	2.86	0.96	6.86	K0IV	4.63	4.61	<1			8175	24
177 389	2.48	0.90	5.31	K0III	4.62	4.56	1.4			41	28
179 799	2.35	0.98	6.54	K0	4.63	4.62	<1			2521	18
187 195	1.29	1.23	6.00	K5III	5.13	4.86	3.1			1735	33
189 319	−1.11	1.57	3.51	K5III	5.14	5.25	−−			133	27
190 608	1.61	1.06	5.09	K2III	4.74	4.69	1.3	1.0	(c)	52	23
197 635	0.56	1.12	5.42	K0III	4.81	4.75	1.4			−−	<4
198 232	−0.44	1.00	4.90	G7III	5.03	4.65	3.7			−−	<4
198 431	1.45	1.08	5.87	K1III	4.71	4.71	<1			89	4
199 665	1.20	0.93	5.52	G6III	4.90	4.59	3.3			−−	<4
217 428	−0.24	0.87	6.23	G4III	5.68	4.54	6.50			−−	<4
218 527	0.76	0.89	5.43	G8III	5.03	4.55	4.1			2863	7
219 615	0.67	0.92	3.69	G7III	4.91	4.58	3.4	1.6	(c)	64	8
224 533	0.70	0.93	4.88	G9III	4.93	4.59	3.4			161	65

−− : no results.
(a) Gray (1989).
(b) Gray (1986).
(c) CORAVEL measurements (de Medeiros & Mayor 1999).
(d) Fekel (1997).
(e) de Medeiros et al. (2002b).

projected rotational velocities. In this case the broadening of the spectral line is dominated by macroturbulence which could differ slightly between stars, even if they have the same color. A more accurate measurement of the $v_{rot}\sin i$ for slowly rotating stars requires spectra taken at much higher spectral resolution, as well as the use of Fourier techniques which are better suited for disentangling the effects of macroturbulence from rotation.

Nineteen of our targets have published rotational velocities, which are given in Cols. 9 and 10 of Table 1. The agreement between the FEROS and the previously published $v_{rot}\sin i$ is excellent, with peak deviations below 1 km s^{-1}. For most stars with $B-V > 1.2$ the derived rotational velocity is negative because $\sigma_{CCF} < \sigma_0$ and they are indicated in Table 1 with the value "−−". Melo et al. (2001) also noticed this effect in their sample, but they could not find any obvious cause in their calibration. This indicates that most likely the rotation rates of the coolest stars are slightly underestimated, and that the estimated error (1 km s^{-1}) should be used as an upper limit for the rotational velocity of these objects. However it seems clear that none of these stars has significant rotation rates.

In Fig. 3 we plot the $v_{rot}\sin i$ against the color index $B-V$, except for those stars with undetermined $v_{rot}\sin i$. All of our stars are slow rotators, with the highest rotation rate being less than 7 km s^{-1}. As observed by other authors (de Medeiros & Mayor 1991), rotation drops quite abruptly with color among F to early G giants and supergiants: at about $B-V \sim 0.7$ for

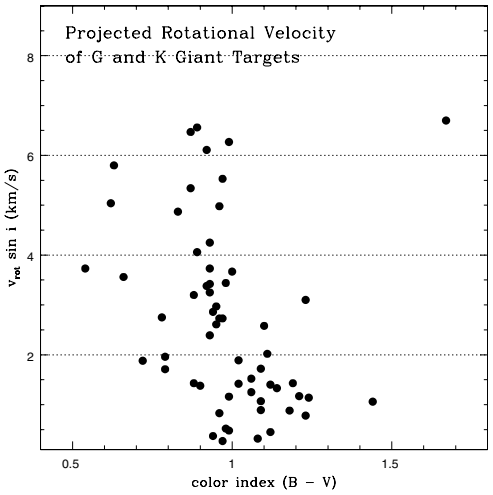

Fig. 3. Projected rotational velocity and rotational period. The −− values in Table 1 (undetermined $v_{\rm rot} \sin i$) are not plotted.

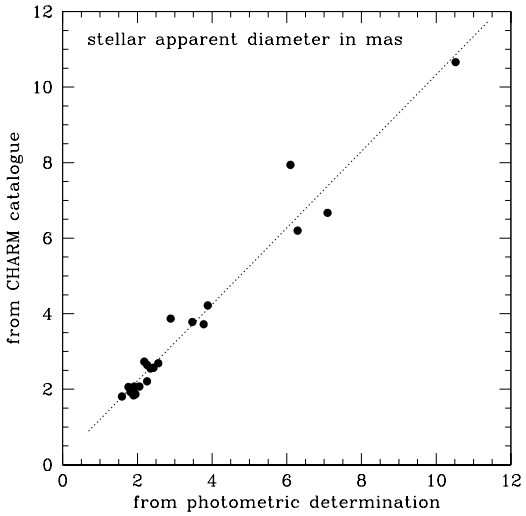

Fig. 4. Comparison of the stellar radii derived from the photometric determination and the values from the CHARM catalogue. The values are in an excellent agreement.

Table 2. Angular diameter, stellar radius and rotational period.

HD	Θ^a	Θ^b	d	$R/R_\odot$ [c]	$P_{\rm rot}/\sin i$
	mas	mas	pc		day
21 120	2.64	2.26	64.85	18.4	143
22 663	2.06	1.76	67.20	14.9	533
23 319	2.73	2.18	54.53	16.0	569
27 371	2.69	2.56	47.24	13.6	253
27 697	2.57	2.43	46.97	12.9	190
32 887	6.20	6.29	69.49	46.3	>2357
47 536	1.81	1.59	121.36	23.6	625
50 778	4.22	3.88	77.28	35.5	>1807
61 935	2.55	2.35	44.33	12.1	326
62 902	1.84	1.90	73.10	14.4	>733
63 697	1.99	1.89	77.70	16.6	>845
65 695	2.07	1.92	76.57	17.1	>870
81 797	10.66	10.52	54.35	62.3	2991
90 957	1.87	1.95	118.76	23.9	>1217
99 167	3.72	3.77	111.73	44.7	>2775
110 014	2.21	2.26	97.66	23.2	1036
113 226	3.78	3.47	31.35	12.7	173
115 478	1.93	1.81	91.41	18.9	>962
124 882	3.87	2.89	85.47	35.6	>1812
125 560	2.07	2.05	58.41	13.0	848
151 249	7.94	6.09	96.06	82.0	>4174
189 319	6.67	7.09	84.03	60.2	>3064

[a] CHARM catalogue (Richichi & Percheron 2002).

[b] This work.

[c] Computed using $\Theta^{(a)}$.

For stars with undetermined $v_{\rm rot} \sin i$ we computed the lower limit for $P_{\rm rot}/\sin i$ by assuming $v_{\rm rot} \sin i = 1$ km s^{-1}.

subgiants/giants and somewhat redward for bright giants and supergiants.

Single giants blueward of this spectral region present a wide range of rotational velocity, from about a few km s^{-1} to about a hundred times the solar rotation. The large majority of single giants redward of this spectral type are essentially slow rotators, with $v_{\rm rot} \sin i$ ranging from about 1 to about 7 km s^{-1}. Among giant stars with spectral types G-K only those in short-period binary systems show enhanced rotation that is due to tidal spin-up from the companion. What we see in Fig. 3 is the expected distribution of the rotational velocity of single G and K giants at the same color interval, with $v_{\rm rot} \sin i$ ranging from 1 to 7 km s^{-1}.

From Fig. 3 we see that only one star with $B-V \geq 1$ that has a significant amount of stellar rotation. This star, HD 78647, is our coolest and intrinsically brightest star with an absolute magnitude of ∼−4. This object is a supergiant which probably also has a larger intrinsic macroturbulent line broadening (see Gray 1989). Its color is also far out of the range of application of the Melo et al. (2001) calibration. For all these reasons its high rotational velocity should be considered as an upper limit.

As far as radii are concerned, for 22 stars from our sample interferometric measurements of apparent diameters are available from the CHARM catalogue (Richichi & Percheron 2002). Given our sample selection of bright, nearby K giants this high rate is not surprising. Indeed, with typical apparent diameters of ∼2 mas our sample provides excellent targets for interferometers. These values can therefore be used to calculate the projected rotational periods $P_{\rm rot}/\sin i = 2\pi R/(v_{\rm rot} \sin i)$. Furthermore, for the stars with known interferometric angular diameter (Table 2) we derived the stellar radii and angular diameter by using the relations of bolometric corrections, effective temperature, and color indexes adopted from Flower (1996). Figure 4 shows a comparison between our diameter computation and the measured angular diameters. The linear fit is given by:

$$\Theta_{\rm CHARM} = (1.014 \pm 0.045)\Theta_{\rm photo} + (0.188 \pm 0.177). \quad (3)$$

Our photometric angular diameter determination is consistent with the obtained values from the CHARM catalogue.

4. Results from RV measurements

The main aim of our survey is to determine any trends in intrinsic RV variability with macroscopic stellar parameters using a statistically large sample that covers a significant fraction of the giant branch in the H-R diagram. To carry out this analysis, however, we must first identify those stars whose RV variability arises due to companions. For stellar companion this task is fairly simple as these produce relative large RV amplitudes generally larger than a few km s^{-1}.

In fact, the other possible causes of long-term RV variations, such as surface inhomogeneities or pulsations usually produces significantly lower RV amplitudes. For example, for spotted stars with $v_{\rm rot} \sin i < 10$ km s^{-1} the RV amplitude due to a 5% starspot filling factor is a few hundred m s^{-1} (see Hatzes 2002). Stars with much larger spots, or high amplitude pulsations should produce significant photometric variations which would be evident in the HIPPARCOS database.

We find it useful to analyze our results by computing the $\sigma_{\overline{\rm RV}}$ of the stars, as given in Col. 11 of Table 1. Out of the full sample of 83 stars, only 77 are analyzed because for the remaining 6 objects less than 4 spectra could be obtained. Looking at the distribution of all the $\sigma_{\overline{\rm RV}}$ we can immediately see that out of the 77 giants, one star, HD 93257 shows a very low level of RV variability; with 29 m s^{-1} rms indeed it is just slightly above our "constant" star τ Cet. Other 20 stars show little variability, with a level of $\sigma_{\overline{\rm RV}}$ below 50 m s^{-1}, or 2 times our estimated accuracy. Of course we cannot exclude the possibility that these stars are indeed variable, but, unless some clear periodicity emerges, we can only consider them as constant at the moment. From the remaining 56 stars, a clear group distinguishes itself from the others: 11 stars have very large variations (more than 800 m s^{-1}) and these are the best candidates for binaries.

The 45 remaining stars exhibit RV variations which are possibly caused by pulsations, rotation or low-mass and planetary companions (as for HD 47536 and HD 122430 with 76 and 79 m s^{-1} rms respectively). For 14 of these 45 objects we have less than 10 measurement points which is insufficient to classify the nature of their RV variability. Additionally, two stars are known to belong to double (visual) systems. They are HD 27256 and HD 224533.

4.1. Multiple systems

11 stars of our sample show variability above 800 m s^{-1}. Most of these show long-term periodic variations ($P > 100$ days) with amplitudes exceeding several km s^{-1}. These stars are HD 21120, HD 22663, HD 27697, HD 40176, HD 62644, HD 176578, HD 179799, HD 187195 and HD 218527. HD 7672 and HD 156111 also show high amplitude RV variations, but the periods appear to be considerably less than 100 days. In all cases the amplitude of the RV variations are clearly due to stellar companions.

With a sample of 77 objects it is possible to apply some statistics to verify our findings. Among giants in open clusters, the incidence of binaries found in spectroscopic surveys with CORAVEL is 26% (Mermilliod et al. 2001). However, this frequency should be considered as a minimum value, which depends on the precision achieved, the time interval and the number of observations. The number of binaries detections is larger when using instrument with better precision (see e.g. Mayor et al. 2001). The RV precision of FEROS is at least ten times better than CORAVEL.

The binary frequency of red giants is lower than that for solar-type stars, which is given, for instance, in Duquennoy et al. (1991). Among red giants, binaries with periods less than 40 days do not exist due to Roche lobe filling, contact phase and mass transfer episodes when the orbital periods are shorter than the critical Roche period at the red giant tip (Mermilliod & Mayor 1992). In particular, clump red giants which have passed through a state of larger radii fulfilled this condition.

Considering the Mermilliod et al. statistics, we could therefore expect that about 20 objects of our sample have stellar companions. Considering, however, that stars already known as binaries were rejected as part of the selection process, we may expect a lower binary rate in our sample, and 11–13 of 77 (14–17%) seem reasonable.

We cannot exclude the possibility that further observations will reveal additional binary candidates, in particular among those that show considerable RV variability, but their number should be limited. If the above statistics can be applied to our sample (and we believe that this should represent an upper limit) we should miss less than 7 additional binaries, and these should likely be very long period systems, whose multiplicity is still hidden in our measurements due to the limited duration of our survey.

When considering the non-binarity bias in our selection criteria, we can also predict that our multiple systems should likely have a high primary to secondary mass ratio, because binary systems composed by stars of similar masses had a higher probability to be discovered in previous studies, since they will tend to show larger RV variations or are double-lined spectroscopic binaries. For the sake of completeness we show all RV curves of the 13 binary candidates so far identified (Figs. 5–7). For 6 stars we had sufficient measurements to compute orbital solutions. These orbital solutions are shown as a line in Figs. 5 and 6. Orbital elements are listed in Table 3.

HD 156111 showed clear short-term RV variability, but we had too few measurements to be able to derive a period. For these reasons additional measurements were made using the coude echelle spectrograph of the Alfred Jensch 2 m telescope of the Thüringer Landessternwarte Tautenburg (TLS). This was one of the few stars of our target sample which was accessible from TLS which is located in Germany. This spectrograph is a grism-crossed dispersed echelle which provides a wavelength coverage of 4750–7070 Å (using the so-called VIS grism) at a resolving power, R ($=\lambda/\Delta\lambda$) = 67 000. An iodine absorption cell placed just before the entrance slit provides the wavelength reference for precise ($\sigma \sim 3$ m s^{-1}) stellar RV measurements. At TLS an additional 13 RV measurements were made which enabled us to determine the period (39.5 days) and to derive an orbit. The right panel of Fig. 6 shows the phase-folded orbital solution to the TLS and FEROS RV measurements.

Figure 8 shows the position of the binaries in the color–magnitude diagram with the same evolutionary track as

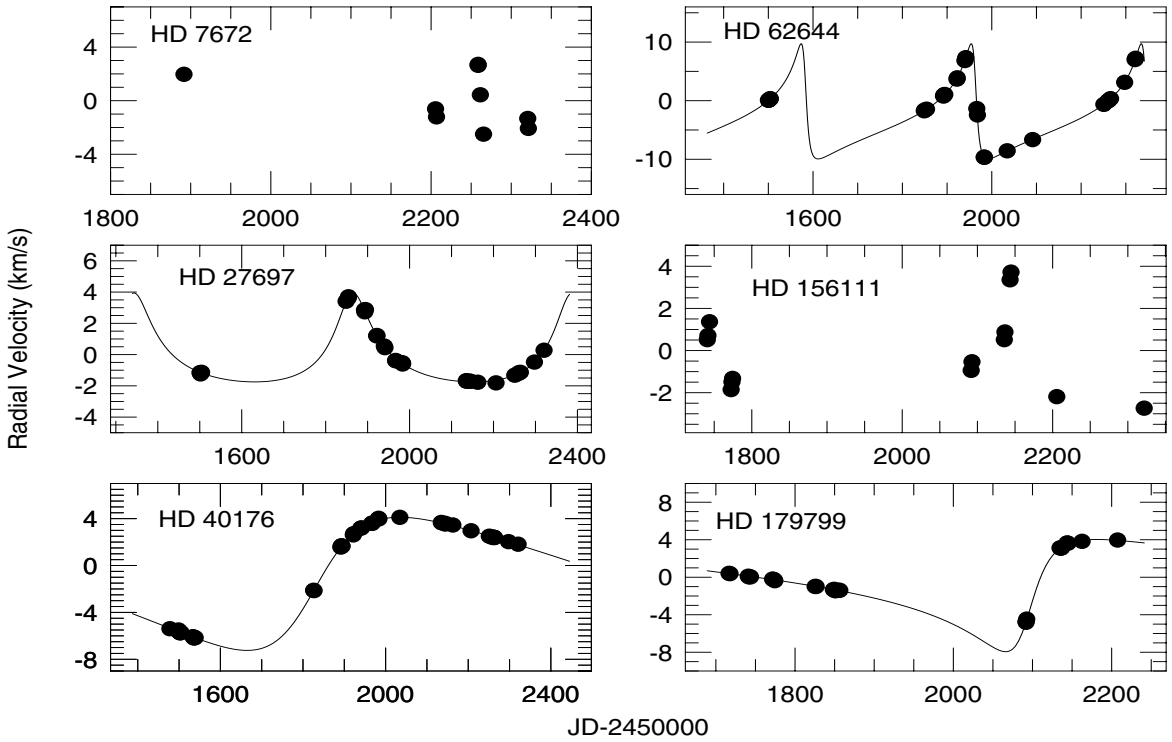

Fig. 5. RV measurements of six binary systems: HD 7672, HD 27697, HD 40176, HD 62644, HD 156111 and HD 179799. The orbital parameters of the Kepler model and the mass-functions are given in Table 3.

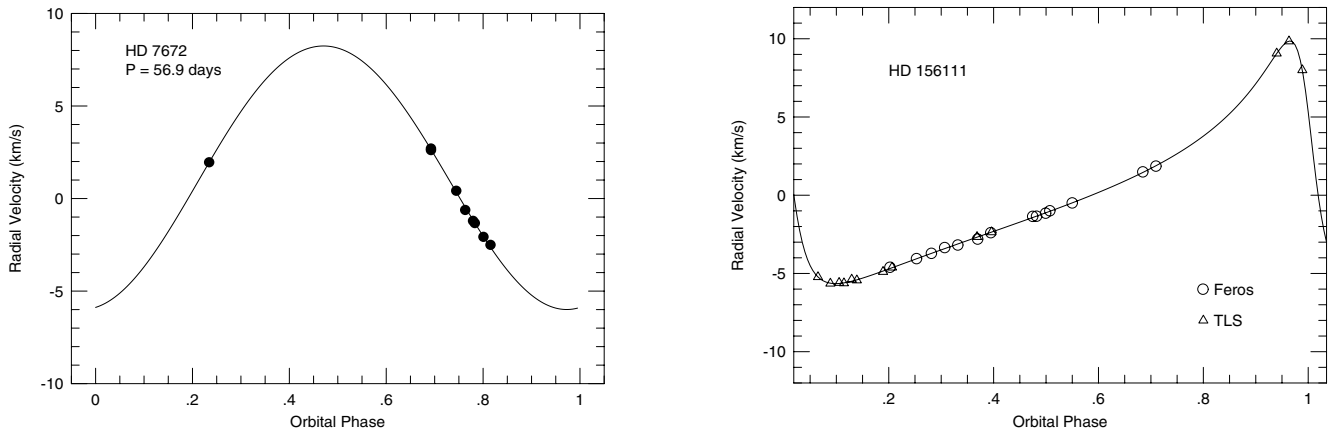

Fig. 6. *Left*: phase folded RV measurements of HD 7672. *Right*: the same for HD 156111 obtained from FEROS and TLS-Tautenburg.

in Fig. 1. For the six binaries with derived orbital elements we adopted primary masses $m_1 = 1.0{-}2.5\ M_\odot$, depending on the star's position in RGB. We computed the mass functions $f(m)$ as given in Col. 5 of Table 3. The resulting companion's masses and the semi-major axes of the orbits are listed in Cols. 6 and 7 of Table 3.

HD 7672 (=AY Cet) was not originally in our program, but was added to increase the number of stars with previously measured rotational velocities. Note that the star has a higher rotation rate than the most targets and our $v_{\rm rot} \sin i$ measurement is in excellent agreement with the result obtained with the Fourier transformation technique (Gray 1989).

Our program provided too few RV measurements to derive an accurate orbit for HD 7672. Our RV measurements showed clear evidence for a $P \approx 60$ d period, but the poor phasing did not allow us to determine the amplitude and eccentricity for the orbit. Fekel & Eitter (1989) presented RV measurements for this star with lower precision ($\sigma \approx 0.5\ {\rm km\,s^{-1}}$). We have combined these with our RV measurements to compute a revised orbit. We found a period of 56.9 days and a circular orbit ($e = 0.02$). Our RV measurements phased to the orbital period along with the orbital solution are shown in Fig. 6 (left panel).

We determined a companion mass of 0.25 $M_\odot$ by assuming a primary mass of 2.5 $M_\odot$. The derived semi-major axis is $a = 0.4$ AU. We estimated a radius of $R \approx 8\ R_\odot$, and when considering the measured rotational velocity results in $P_{\rm rot}/\sin i \approx 75$ days, or comparable to the orbital period, HD 7672 is possibly a tidally locked binary with the same

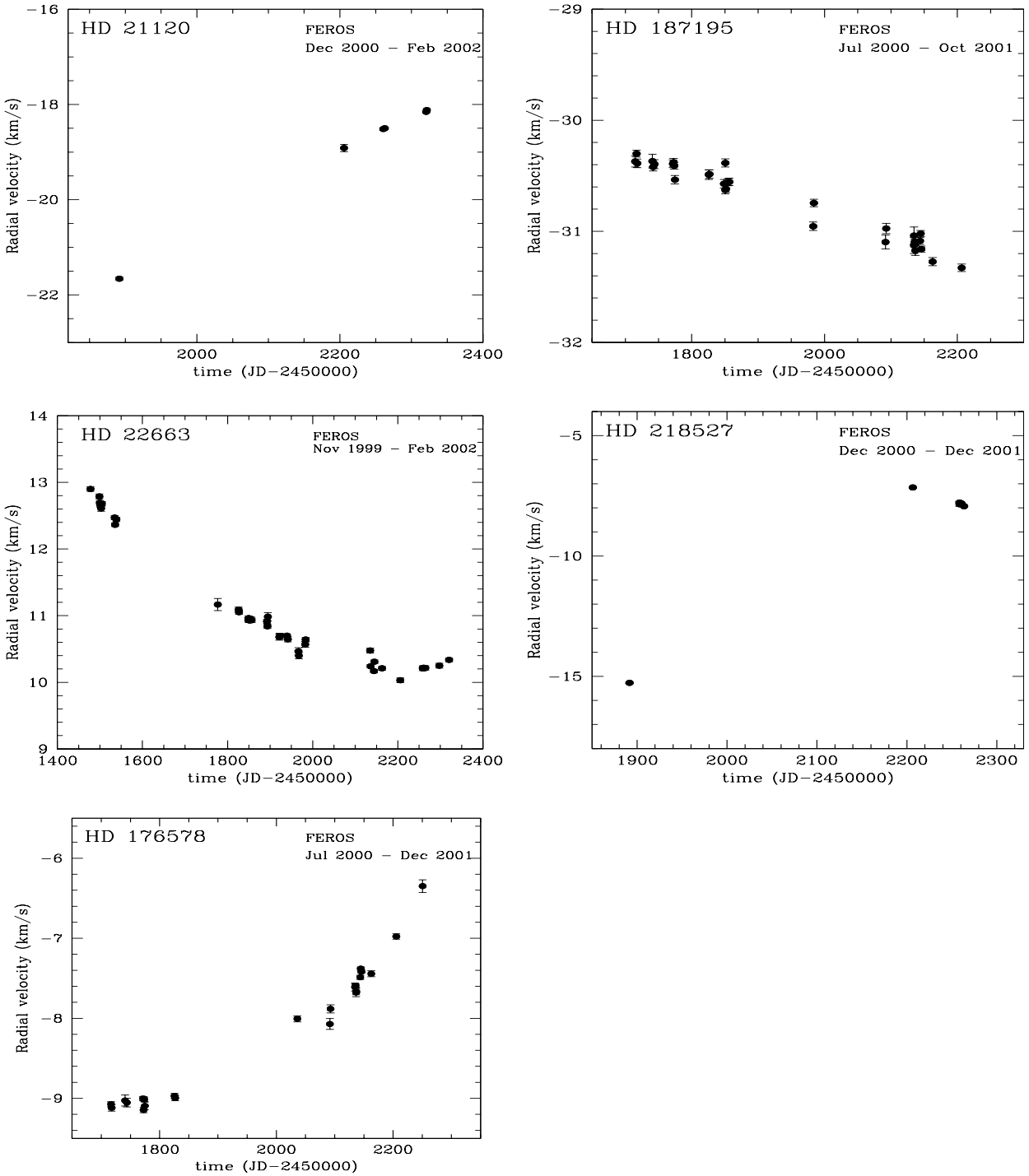

Fig. 7. RV measurements of binary systems HD 21120, HD 22663, HD 176578, HD 187195 and HD 218527. These binaries show much longer period than our total observation span.

orbital and rotational period. For binaries with a red giant primary and $P < 120$ days the circular orbit is due to tidal interaction between the two components (Mermilliod & Mayor 1992).

HD 27697 exhibits an orbital period of $P = 522 \pm 1.8$ days. The period we found is comparable to the 529.8 day period reported in de Medeiros et al. (2002a). We obtained an eccentricity $e = 0.48$. With a semi-amplitude $K_1 = 2.84\,\mathrm{km\,s^{-1}}$ and $m_1 = 2.5\,M_\odot$ we derived a minimum mass of $m_2 \sin i = 0.18\,M_\odot$. The semi-major axis of the orbit is 1.76 AU. With a $P_{\rm rot}/\sin i$ of 190 days, the orbital period is substantially longer than the rotational one.

With a period of 1420.6 days and $K_1 = 5.68\,\mathrm{km\,s^{-1}}$ HD 40176 has a more massive companion than the two giants described above. We derived a minimum mass of $m_2 \sin i = 0.59\,M_\odot$ an eccentricity of $e = 0.39$ and an orbital semi-major axis of 3.60 AU. The systems HD 62644, HD 156111 and HD 179799 each have companions with high eccentric orbits ($e \geq 0.65$). Their orbital periods are 380.6 days (HD 62644), 39.5 days (HD 156111) and 856.1 days (HD 179799).

Table 3. Companions of six binaries.

HD	K_1 [km s^{-1}]	P [days]	e	$f(m)$ [$M_\odot$]	$m_2 \sin i$ [$M_\odot$]	a_2 [AU]
7672	7.11 ± 0.47	56.9 ± 0.1	0.02	2.1×10^{-3}	0.25	0.41
27 697	2.84 ± 0.03	522.1 ± 1.8	0.48	8.4×10^{-4}	0.18	1.76
40 176	5.68 ± 0.04	1420.6 ± 19.8	0.39	2.1×10^{-2}	0.59	3.60
62 644	9.84 ± 0.07	380.6 ± 0.1	0.73	1.2×10^{-2}	0.32	1.20
156 111	7.75 ± 0.02	39.5 ± 0.0	0.65	8.3×10^{-4}	0.10	0.23
179 799	5.99 ± 0.40	856.1 ± 39.1	0.66	8.1×10^{-3}	0.30	2.14

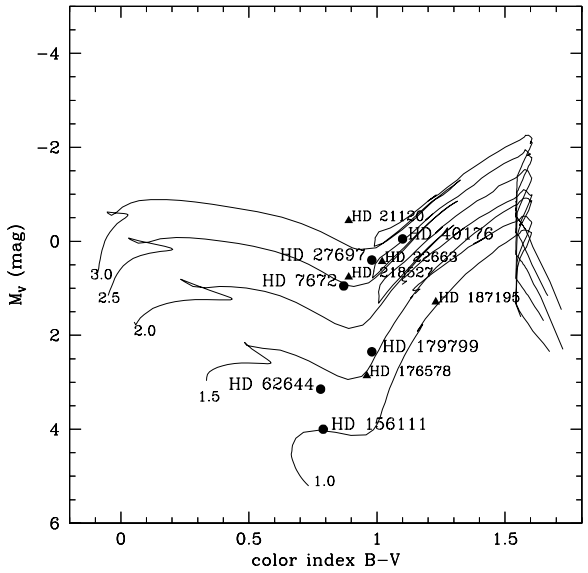

Fig. 8. Color–magnitude diagram of the binaries found. The same evolutionary track as in Fig. 1 has been added. The primary masses can be estimated from the position in this diagram. The dots and triangles represent binaries with and without orbital solutions.

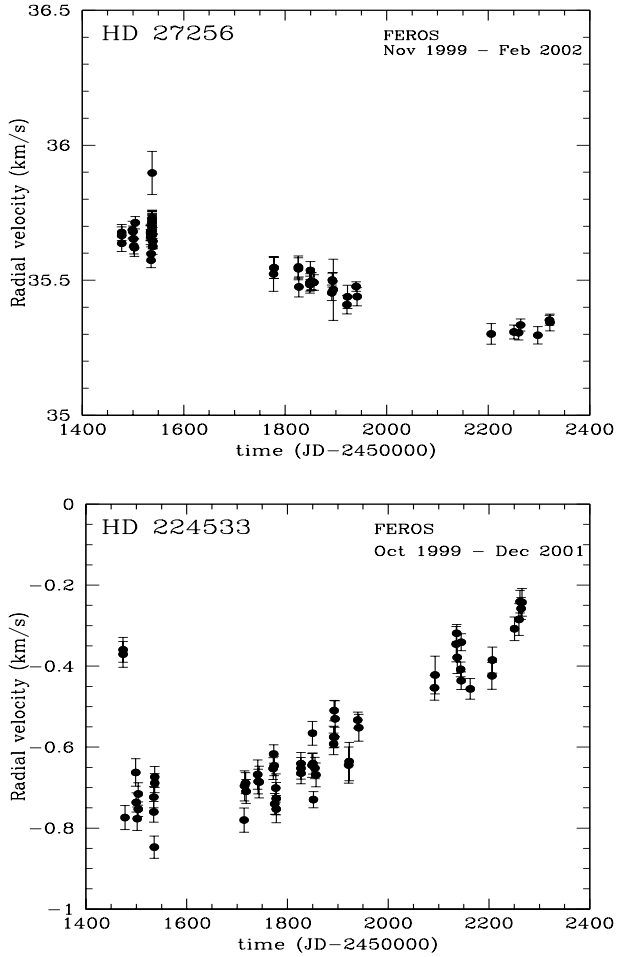

Fig. 9. RV measurements of HD 27256 and HD 224533. These stars are known as stars in visual double systems. However, the measured RV variations are possibly due to other unseen companions.

We obtained $m_2 \sin i = 0.32\ M_\odot$ for HD 62644, 0.10 $M_\odot$ for HD 156111 and 0.30 $M_\odot$ for HD 179799. The semi-major axes are 1.2 AU, 0.23 AU and 2.14 AU, respectively. For HD 156111 which has a stellar radius $R = 1.8\ R_\odot$ and $v_{\rm rot} \sin i = 2.0$ m s^{-1} we compute $P_{\rm rot}/\sin i = 47$ days, which is close to the orbital period. However, it is not clear if this is a tidal-locked system. The rotation velocity is rather low for a synchronized system.

The systems HD 21120, HD 27256, HD 22663, HD 176578, HD 187195, HD 218527 and HD 224533 show orbital periods longer than our total observation timespan, and we would need more time to derive the RV solution for these binaries; we consider this goal is outside the purpose of this project.

We are very interested in the nature of the companions around HD 27256 and HD 224533. The reason is that, although these giants are classified as stars in visual double systems, we found that the RV variations observed are not due to the visual secondary component of the systems. They are instead induced by unseen low-mass, possibly brown dwarf or very low-mass stellar companions. HD 27256 and HD 224533 show low RV variability relative to the other binaries. Their $\sigma_{\overline{\rm RV}}$ values are 136 m s^{-1} and 161 m s^{-1}. The separation of the two components is 48.56 arcsec for HD 27256 (Torres et al. 1986) and 0.945 arcsec for HD 224533 (Horch et al. 1999), with a magnitude difference of respectively, about 8.7 and 5.3 magnitudes.

For HD 27256 which is 50.05 pc far away this implies a separation between the components of ≈2434 AU. Such a large separation requires a long orbital period. Under reasonable assumptions on the mass of the two stars (in the 3 $M_\odot$ range for the primary and about 0.5 for the secondary), the periods required are of the order of 50–100 thousand years, and the associated $K_1 \sim 300$ m s^{-1}. The maximum linear acceleration of the primary due to this companion (assuming a circular orbit) would be about 0.004 m s^{-1} yr^{-1}, or about 5 orders of magnitude smaller than the observed accleration. The observed RV variations cannot be due to the known stellar companion and we are obliged to look for other interpretations. We suggest that the RV variability observed on HD 27256 (see Fig. 9 upper panel) is induced either by another unseen companion or by rotational modulation. In case of an unseen companion, the low $\sigma_{\overline{\rm RV}}$ could imply a sub-stellar object. This star has also been thoroughly studied for stellar activity, being detected in the Ca II chromospheric lines (Pasquini et al. 2000), by EUVE and ROSAT in the soft X-ray. Its chromospheric activity and

rotational velocity are usual for stars of its mass and temperature, and with a radius of about 14.5 $R_\odot$ and a projected rotational velocity in the range of 4.5–6 km s^{-1} the expected rotational period is not longer than 165 days, far shorter than the long period RV variations observed by us. Therefore rotational modulation does not provide a convincing explanation.

In Paper I we discussed HD 224533 based on our 14 months observation data. There we concluded that the RV variability of this giant may be caused by an unseen companion rather than the visible component detected by Horch et al. (1999). Our new data confirms the previous analysis, and, as can be seen in Fig. 9 (lower panel), we have observed a RV variation of ∼600 m s^{-1} within ∼800 days. The mean RV of our measurements for this star is −0.51 km s^{-1}. The published RV of this star is −0.2 km s^{-1} (Duflot et al. 1995). The RV value for τ Cet in the same catalogue is of −16.4 km s^{-1} which differs by about 0.26 km s^{-1} from our mean value. Applying the τ Cet offset to HD 224533, the Duflot RV for this star would become −0.46 km s^{-1}, that is only 50 m s^{-1} above our mean result. There is no evidence for this star of velocity amplitude variations exceeding 1 km s^{-1}. When considering all of the available RV measurements for this star the velocity amplitude cannot be much larger than about 1.0 km s^{-1}. If we assume a primary mass $m_1 = 2\ M_\odot$, a semi-amplitude $K_1 = 0.8$ km s^{-1}, a maximal period of 2000 days (that is about twice of our observation span) and an eccentricity $e = 0.3$, we obtain a maximum $m_2 \sin i \sim 73\ M_{\rm Jup}$. The semi-major axis will be ∼4 AU. The unseen companion around HD 224533 can be a brown dwarf candidate.

In addition to all the binary systems mentioned above we found two stars for which we could produce evidence for planetary companions: HD 47536 (Setiawan et al. 2003b) and HD 122430 (Setiawan 2003c). Not only do these objects show significant periodic variabilities, but, in addition, their RV variabilities are not dependent on stellar activity or bisector variations. Thus, it cannot be ascribed to rotational modulation or pulsations.

4.2. $\sigma_{\overline{\rm RV}}$ trend along the RGB

Figure 10 is the H-R diagram of the sample stars. The size of the symbols for the single stars is proportional to their variability.

In Paper I we suggested that the variations in RV observed were broadly correlated with the position of the star in the H-R diagram. Is this variation still present in our "cleaned" sample, that is, after binaries have been eliminated? A glance at Fig. 10, in which the size of the dots is proportional to the RV variations, seems to confirm this trend: going towards more luminous stars, the circles tend to be bigger. For the lower part of the RGB, a typical $\sigma_{\overline{\rm RV}}$ – with the exception for 3 stars – is less than 40 m s^{-1}. In the middle, including the clump region, $\sigma_{\overline{\rm RV}}$ = 40–60 m s^{-1} are measured for the most targets. In the upper region larger $\sigma_{\overline{\rm RV}}$ are detected up to 301 m s^{-1}. Figure 11 illustrates examples of RV measurements of giants in the lower (HD 92588), middle (HD 61935) and upper (HD 81797) regions of the RGB. The increase of $\sigma_{\overline{\rm RV}}$ along the RGB is

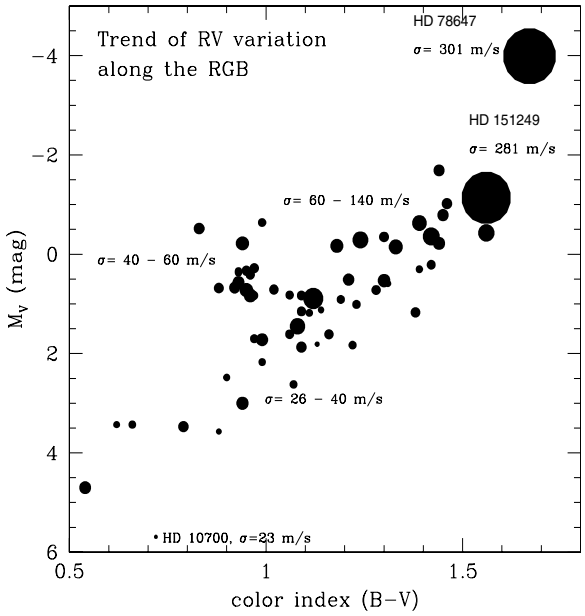

Fig. 10. Trend of RV variation – given by $\sigma_{\overline{\rm RV}}$, listed in Table 4 – along the RGB. The scale of the dots gives the $\sigma_{\overline{\rm RV}}$ value. The $\sigma_{\overline{\rm RV}}$ in the upper part of the RGB is significantly larger than those in the lower and middle part as well as in the clump region. The cool luminous giant HD 151249 and the supergiant HD 78647 have the largest RV variabilities (see text).

consistent with the RV survey reported by Mitchell et al. (2001) for a sample of 182 K giants.

We found it instructive to plot the RV measured variability as a function of the absolute stellar magnitude, as done in Fig. 12. In this figure we have only considered the "single" stars, plus the two low amplitude binaries, HD 27256 and HD 224533 (plotted as dots), HD 47536 and HD 122430, the stars with planetary candidates (plotted as filled triangle). The lower envelope of the data points suggests that the minimum level of RV variability increases with the stellar luminosity; that is, no bright giant is constant at the 25 m s^{-1} accuracy of our survey. Also, the degree of variability seems to increase with luminosity, since the spread of the data increases with magnitude. Both these results could indicate the dependence of RV variability on some basic stellar parameter, such as gravity. The presence of the two binary systems, however, calls for a cautious interpretation: they both lie in the upper envelope distribution and this could suggest that several of the stars in the upper envelope of the diagram are multiple systems. The evidences for planetary companions to HD 47536 and HD 122430 (marked with triangles) in the upper envelope of the distribution, but still in a quite crowded portion of the diagram, confirm that the presence of planetary companions is also an attractive explanation for the upper part of the distribution. By excluding stars with stellar companions, the average of all $\sigma_{\overline{\rm RV}}$ is 60 m s^{-1}.

We note that two of our targets: HD 78647 and HD 151249 show $\sigma_{\overline{\rm RV}}$ = 301 and 281 m s^{-1}, respectively. The RV variability of HD 78647 is of long-period and this star is by far the brightest and coolest of the sample, corresponding to a late K supergiant. Our preliminary investigation of their

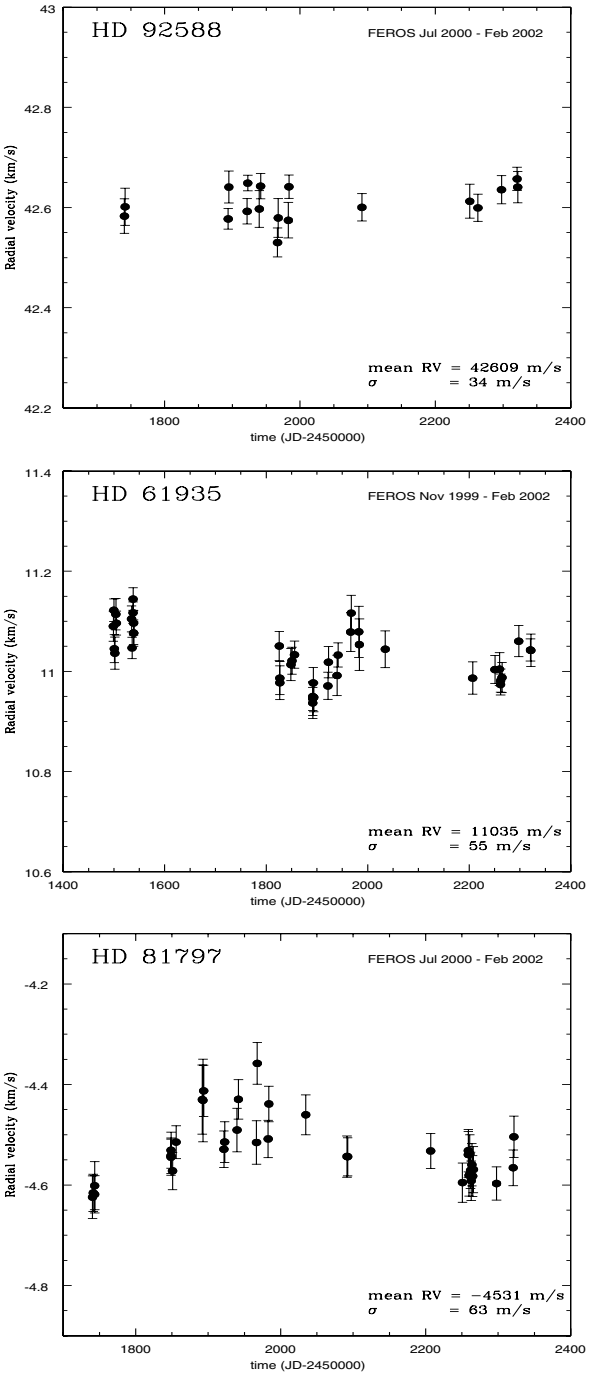

Fig. 11. 3 stars from different RGB regions are presented. HD 92588 – located in the lower of RGB – with $\sigma_{\overline{\rm RV}}$ less than 40 m s^{-1}, HD 61935 represents stars in the middle of RGB with $\sigma_{\overline{\rm RV}}$ = 40–60 m s^{-1} and HD 81797 on the upper part of RGB with $\sigma_{\overline{\rm RV}} > 60$ m s^{-1}.

chromospheric activity through the analysis of the Ca II K emission reveals a measurable variability in these lines, possibly in phase with the RV measurements, and this would clearly favour the interpretation that their long-period RV variability is due to rotational modulation rather than due to sub-stellar companions. In addition, we observed for HD 78647 a correlation between the RV measurements and the bisector velocity span (see Queloz et al. 2001), shown in Fig. 13. As far as HD 151249 is concerned, the data available for this star are

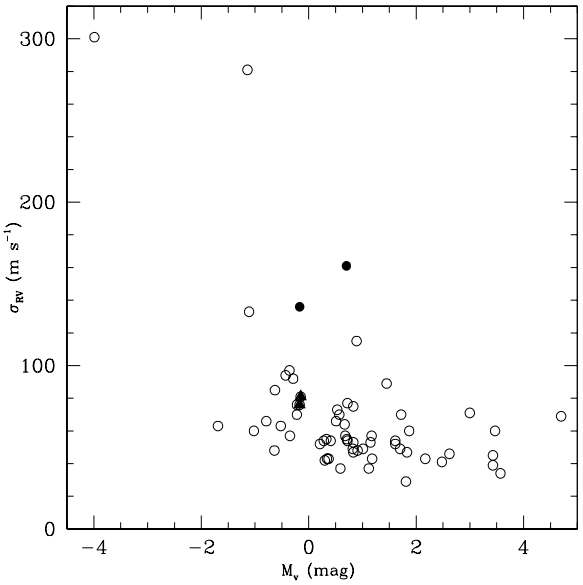

Fig. 12. RV variability as a function of the stellar magnitude for the stars of our sample, after eliminating the stars with bona fide stellar companions. The two binaries with possible sub-stellar companions (HD 27256 and HD 224533) are given as dots, whereas stars hosting giant planet candidates HD 47536 and HD 122430 are indicated with filled triangles. Note the increase of spread and of minimum variability with increasing luminosity.

unfortunately insufficient to derive a full orbital analysis. However, we could observe a slight correlation between the time variation of the relative intensity ratio Ca II K2V/K2R with the RV. A complete chromospheric and bisector analysis of the whole sample is beyond the scope of this study and will be presented elsewhere. It is worth noting that if the variability in HD 78647 is indeed caused by the rotational modulation of surface inhomogeneities, this star may be an excellent target for a large interferometer.

5. Conclusions

We report the results of our study of RV variability of G and K evolved stars, and we have so far analyzed high resolution spectra for 77 giants. By using the G dwarf τ Cet as a calibrator we obtained a precision of $\sigma_{\overline{\rm RV},\tau\,{\rm Cet}} = 22.8$ m s^{-1} over this period.

More than 70% of the sample stars reveal variability over 50 m s^{-1} and can be considered bona fide variable. This definitely confirms that RV variability among G and K giants is ubiquitous. Based on our sample, we produced evidence that 11 stars belong to binary/multiple systems. For 6 of the 11 systems we derived the minimum masses of the companions $m_2 \sin i$ between 0.1–0.6 $M_\odot$. We showed that the variabilities observed in 2 additional giants, known as visual binaries, are not induced by the visual companions, but rather by unseen objects, which might be in the brown dwarf mass regime. When considering that our sample was already selected to avoid known binary stars, the statistics of binary objects is consistent with surveys among binaries in main sequence stars and binaries with red giant primary. The mass distribution shows many low-mass companions, and this is also in qualitative agreement with

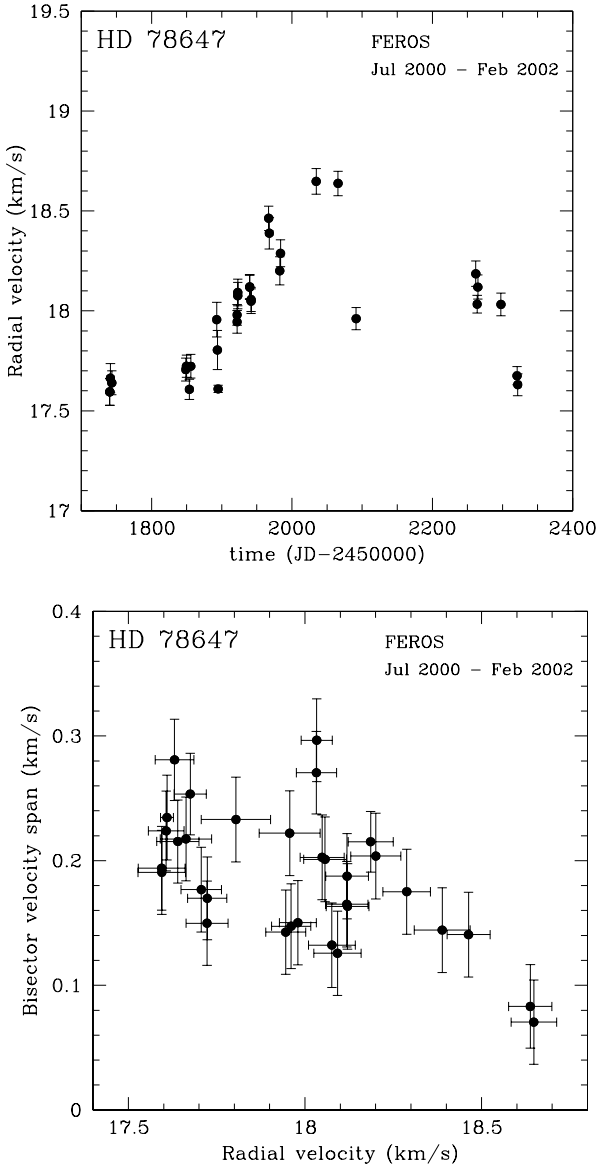

Fig. 13. The upper panel shows the RV measurements of HD 78647. The lower panel presents the bisector velocity spans vs. the RV measurements. A clear correlation is present; together with variability detected in the Ca II K line, this indicates that the RV variability is induced by rotational modulation.

our selection bias. Two stars from our sample, HD 47536 and HD 122430 show evidence of planetary companions. The presence of stellar/sub-stellar companions seems therefore to represent a relevant component in the RV variability of giant stars.

Once the known binaries were eliminated from the analysis, we found that our sample stars exhibit typical RV variability of $\sigma_{\overline{\mathrm{RV}}} = 60\ \mathrm{m\,s^{-1}}$. This average RV is about a factor of 3 greater than the spectrograph precision. Our results allowed us to establish a relationship between RV variability and position in the RGB. Stars in the upper region of the RGB exhibit considerable RV variations with $\sigma_{\overline{\mathrm{RV}}} > 60\ \mathrm{m\,s^{-1}}$, whereas in the other regions $\sigma_{\overline{\mathrm{RV}},\tau\,\mathrm{Cet}} < \sigma_{\overline{\mathrm{RV}}} < 60\ \mathrm{m\,s^{-1}}$. This result can be seen in more detail by plotting the RV variability as a function of the stellar absolute magnitude. In this diagram we can see how the minimum level of variability increases with the stellar luminosity, as well as the spread in variability. The presence of the low-mass binaries in the upper envelope of the distribution may suggest that low-mass companions can still be discovered. However, companions cannot explain the whole range of variability observed, which must be induced by other causes as well.

For the two most luminous and coolest stars, our Ca II and bisector analysis shows that the large RV variability observed (around 300 $\mathrm{m\,s^{-1}}$) is likely associated with chromospheric activity, and therefore rotational modulation is the cause of RV variability. They deserve further study and they would be excellent candidates for large interferometers observations.

Finally, the reason for the RV variability for the bulk of the 45 remaining stars is still unknown, and will have to wait for the ongoing chromospheric and bisector analysis to derive some firm conclusions. The observed growth of the variability with stellar luminosity is certainly consistent with the expectation of oscillations, in that, in general, more luminous stars will have lower gravities. Despite the brightness of our sample stars, very few have measured metallicities, while the knowledge of the star metallicity is necessary to attempt a detailed analysis of stellar masses, radii and gravities because of the well-known degeneracy affecting mass and metallicity in the colors of RGB stars. Pending a more accurate mass determination for each star, which will be attempted after a detailed chemical analysis of the objects (da Silva et al. 2004, in preparation) we can say that, with a variability of about 80 $\mathrm{m\,s^{-1}}$ at $M_V \sim -0.5$ and 40 $\mathrm{m\,s^{-1}}$ at two magnitudes fainter, and assuming the same mass for the objects, this would lead to a difference in gravity of about a factor of 12 (considering both stars on the RGB); this would imply only a mild dependence of the RV variability on gravity, at least in these regimes.

Concerning the possibility that other mechanisms are responsible for the observed RV, we can only say that at least in two luminous and coolest giants we observed chromospheric variations associated which RV variations, which indicates that rotational modulation may be relevant. The observed dependence is smaller than what is predicted for instance by Kjeldsen & Bedding (1995).

Acknowledgements. We are grateful to A. Torrejon and R. Vega for their assistance during the observation. We thank E. Guenther for observing our target with the TLS-Tautenburg telescope. J. Setiawan thanks the state Baden-Würtemmberg for the grant through the Landesgraduiertenförderungsgesetz. L. da Silva and J. R. de Medeiros thank the CNPq Brazilian Agency for the continuous financial support. G. Caira helped in the analysis of the data, and her work was supported through ESO DGDF. We thank J. Eskdale and M. Pia for a careful reading of the manuscript.

References

Barban, C., Mitchel, E., Martic, M., et al. 1999, A&A, 350, 617
Baranne, A., Queloz, D., Mayor, M., et al. 1996, A&AS, 119, 373
Benz, W., & Mayor, M. 1984, A&A, 138, 183
Bedding, T. R., Butler, R. P., Kjeldsen, H., et al. 2001, ApJ, 549, L105
Bouchy, F., & Carrier, F. 2001, A&A, 374, L5
Brown, T., Gilliland, R. L., Noyes, R. W., et al. 1991, ApJ, 368, 599

Butler, R. P., Marcy, G. W., Williams, E., et al. 1996, PASP, 108, 500
Butler, R. P., Tinney, C. G., Marcy, G. W., et al. 2001, ApJ, 555, 410
Buzasi, D., Catanzarite, J., Laher, R., et al. 2000, ApJ, 532, L133
Campbell, B., & Walker, G. A. H. 1979, PASP, 91, 540
Cochran, W. D., & Hatzes, A. P. 1990, SPIE, 1318, 148
da Silva, L., et al. 2004, in preparation
Duflot, M., Figon, P., & Meyssonnier, N. 1995, A&AS, 114, 269
Duquennoy, A., & Mayor, M. 1991, A&A, 248, 485
Fekel, F. C., & Eitter, J. J. 1989, AJ, 97, 1139
Fekel, F. 1997, PASP, 109, 514
Flower, P. J. 1996, ApJ, 469, 355
Frandsen, S., Carrier, F., Aerts, C., et al. 2002, A&A, 394, L5
Frink, S., Mitchell, D. S., Quirrenbach, A., et al. 2002, ApJ, 576, 478
Girardi, L., Bressan, A., Bertelli, G., & Chiosi, C. 2000, A&AS, 141, 371
Gray, D. F. 1976, The Observation and Analysis of Stellar Photosphere
Gray, D. F., & Toner, C. G. 1986, ApJ, 310, 277
Gray, D. F. 1989, ApJ, 347, 1021
Hatzes A. P., & Cochran, W. D. 1993, ApJ, 413, 339
Hatzes A. P., & Cochran, W. D. 1994, ApJ, 422, 366
Hatzes A. P., & Cochran, W. D. 1996, ApJ, 468, 391
Hatzes A. P. 2002, AN, 323, 392
Hatzes A. P., Cochran, W. D., Endl, E., et al. 2003, ApJ, 599, 1383
Horch, E., Ninkov, Z., van Altena, W. F., et al. 1999, AJ, 117, 548
Kaufer, A., & Pasquini, L. 1998, SPIE, 3355, 844
Kjeldsen, H., & Bedding, T. R. 1995, A&A, 293, 87
Larson, A. M., Irwin, A. W., Yang, S. L. S., et al. 1993, PASP, 105, 332
Marcy, G., & Butler, P. 1996, ApJ, 464, L147
Mayor, M., & Queloz, D. 1995, Nature, 378, 355
Mayor, M., Udry, S., Halbwachs, J. L., & Arenou, F. 2001, in The Formation of Binary Stars, ed. H. Zinnecker, & R. D. Mathieu, IAU Symp., 200
Melo, C. H. F., Pasquini, L., & de Medeiros, J. R. 2001, A&A, 375, 851
de Medeiros, J. R., & Mayor, M. 1999, A&AS, 139, 433
de Medeiros, J. R., da Silva, J. R. P., & Maia, M. R. G. 2002a, ApJ, 578, 943
de Medeiros, J. R., Udry, S., Burki, G., & Mayor, M. 2002b, A&A, 395, 97
Merline, W. J. 1995, Ph.D. Thesis, The University of Arizona, Tucson, AZ
Mermilliod, J. C., & Mayor, M. 1992, in Binaries as Tracers of Stellar Formation, ed. A. Duquennoy, & M. Mayor (Cambridge University Press)
Mermilliod, J. C., Claria, J. J., Andersen, J., et al. 2001, A&A, 375, 30
Mitchell, D. S., Frink, S., Quirrenbach, A., et al. 2001, AAS, 199, 9203
Pasquini, L., Brocato, E., & Pallavicini, R. 1990, A&A, 234, 277
Pasquini, L., de Medeiros, J. R., & Girardi, L. 2000, A&A, 361, 1011
Pepe, F., Mayor, M., Delabre, B., et al. 2000, SPIE, 4008, 582
Queloz, D., Allain, S., Mermilliod, J. C., et al. 1998, A&A, 335, 183
Queloz, D., Henry, W., Sivan, J. P., et al. 2001, A&A, 379, 279
Richichi, A., & Percheron, I. 2002, A&A, 386, 492
Sato, B., Hiroyasu, A., Eiji, K., et al. 2003, ApJ, 597, L57
Setiawan, J., Pasquini, L., da Silva, L., et al. 2000, The Messenger, 102
Setiawan, J., Pasquini, L., da Silva, L., et al. 2003a, A&A, 397, 1151
Setiawan, J., Hatzes, A., von der Lühe, O., et al. 2003b, A&A, 398, L19
Setiawan, J. 2003c, in Towards Other Earths, DARWIN/TPF and the Search for Extrasolar Terestrial Planets, held in Heidelberg, Germany, 22–25 April, ESA SP-539, ed. M. Fridlund, & T. Henning, 595
Smith, P. H., McMillan, R. S., & Merline, W. J. 1987, ApJ, 317, L79
Torres, G. 1986, A&AS, 64, 105
Walker, G. A. H., Yang, S., Campbell, B., et al. 1989, ApJ, 343, L21